16th World Conference on Earthquake Engineering, 16WCEE 2017
Santiago Chile, January 9th to 13th 2017
Paper N° 116
Registration Code: S-I1462378871

THE SEISMIC RESPONSE OF EMBEDDED COLUMN BASES – TESTS AND STRENGTH MODEL

D.A. Grilli[(1)], A.M. Kanvinde[(2)]

[(1)] *Associate, Wiss Janney Elstner Associates, Inc., dagrilli@ucdavis.edu*
[(2)] *Professor and Chair, University of California, Davis, kanvinde@ucdavis.edu*
…

Abstract

Embedded Column Base (ECB) connections are commonly used in mid- to high-rise moment frame buildings, when exposed base plate connections cannot economically provide adequate strength or stiffness. Results from five full-scale tests on ECB connections are presented to examine their seismic response. The tests indicate that (similar to composite beam column connections), response is controlled by a combination of the following mechanisms: (1) bearing of the column flanges against the concrete, (2) panel zone shear, and (3) vertical restraint to uplift and rotation of the embedded base plate. A new strength model is presented. The model considers these mechanisms, as well as their interactions. Limitations of the research are discussed along with their implications for design.

Keywords: base connection; column base; embedded steel; composite connection; base plate

1. Introduction

For tall buildings with where large column base moments must be resisted by the footing, designers often use "embedded" type base connection (see Fig. 1), in which the dominant mechanism of moment resistance is direct bearing between the column and the concrete footing. Significant research has been conducted on exposed type base connections, where the base plate is anchored on top of the footing [1], [2]; however similar research is not available for Embedded Column Base (ECB) connections, such that there are no established approaches to facilitate their design – specifically, AISC Design Guide One [3], and the SEAOC SSDM [4] exclusively address exposed type connections. For the design of ECB connections, practitioners use ad hoc methods based on research on other structural components that show mechanisms similar to those expected in ECB connections, including steel coupling beams in shear walls and composite beam-column connections. However, these components have significant differences with respect to ECB connections, making such adaptation somewhat challenging. Specifically, these pertain to the presence of column axial force and indeterminate interactions between the horizontal bearing and the vertical bearing mechanisms that are shown in Fig. 1. Motivated by these issues, this paper presents results from 5 full-scale tests on embedded column base connections representing typical column base connections for moment-frame buildings, such that their failure is controlled by interactions of flexure and axial load. The paper presents these experimental results and briefly outlines a working model for the strength characterization and design of such connections.

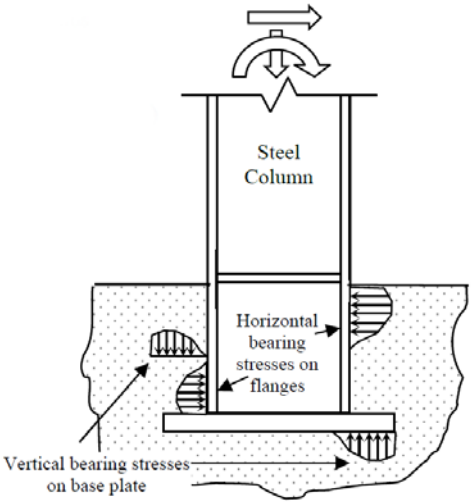

Fig. 1 – Load transfer in ECB Connections

2. Experimental Program

All tests specimens were cantilever columns loaded laterally in deformation control as per a cyclic loading protocol. This protocol was applied under a constant axial load (either compressive, tensile, or zero). The major variables interrogated were (1) embedment depth (2) column size, including flange width, and (3) axial load. Table 1 summarizes the test matrix, along with key experimental results, whereas Fig. 2 shows the test setup with specimen being tested (including both tension and compression setups).

Table 1 – Test matrix

Test #	Column Size, (b_f[mm])	Axial load, P [kN]	d_{embed} [mm]	Base Plate, $t_p \times N \times B$ [mm]	z [m]	M_{base}^{max} [kN-m]
1	W14x370 (419)	445 (C)	508	$51 \times 762 \times 762$	2.84	2579(+)
						2613(-)
2	W18x311 (305)			$51 \times 864 \times 711$		2324(+)
						2168(-)
3	W14x370 (419)	0	762	$51 \times 762 \times 762$	3.10	3741(+)
						3444(-)
4		445 (C)				4124 (+)
						3612(-)
5		667 (T)				3800 (+)
						3464(-)

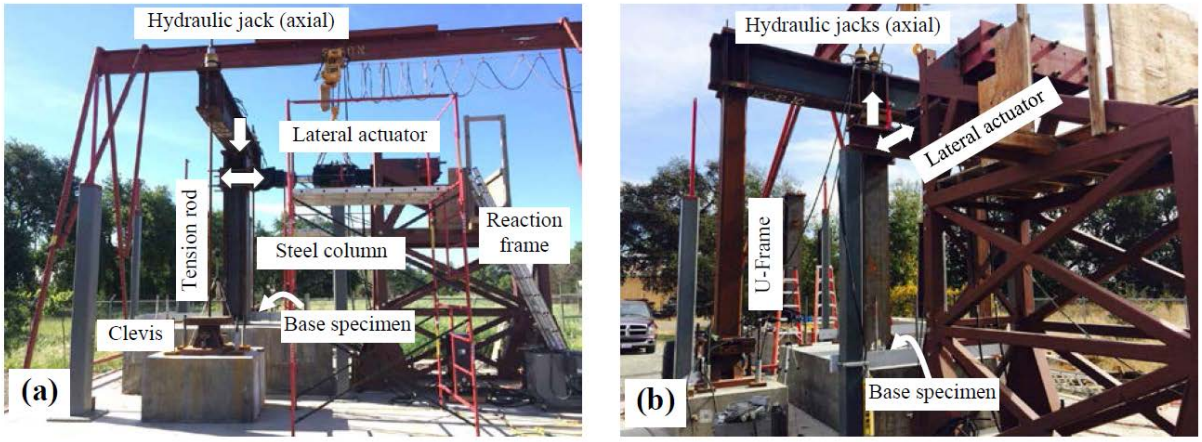

Fig. 2 – Test setup for (a) specimens with axial compression and (b) specimens with axial tension

All specimens reflected current construction practice. Fig. 2a and b show photographs of the test setup for compressive load (Test #1, 2, 4) and tensile axial load (Test #5) respectively. Test #3, which has no axial load, does not have the fixtures for introduction of axial load, which are present in the other tests. Main features of the test setup and specimens are described in [5].

Table 1 summarizes the test matrix. The parameters varied include: (1) the embedment depth, (2) axial load, and (3) the column size. The values for each of these were selected based on a consideration of similarity to full-scale connections, and limitations of the test setup. For all the tests, displacement-controlled cyclic lateral loading was applied according to the SAC loading protocol [6] to represent deformation histories consistent with seismic demands in moment frame buildings.

3. Test results

Fig. 3a-e show the moment-drift plots for all the specimens, whereas Fig. 4 shows photographs of damage and failure. All experiments followed a qualitatively similar progression of damage, with some variations. Small cracks began to form near the corners of the column immediately after the commencement of lateral loading, but this did not affect the load-deformation response, such that linear elastic response was observed until 0.5% drift. After this, gradual nonlinearity in the load deformation curve was observed, accompanied by the opening of a small gap adjacent to the tension flange, accompanied by the growth of the diagonal cracks described previously. This was accompanied by strength degradation as well as pinching response. The pinching response is due to the gapping shown in Fig. 4b resulting in unrestrained movement of the column within its "socket," as it moved through the vertical position.

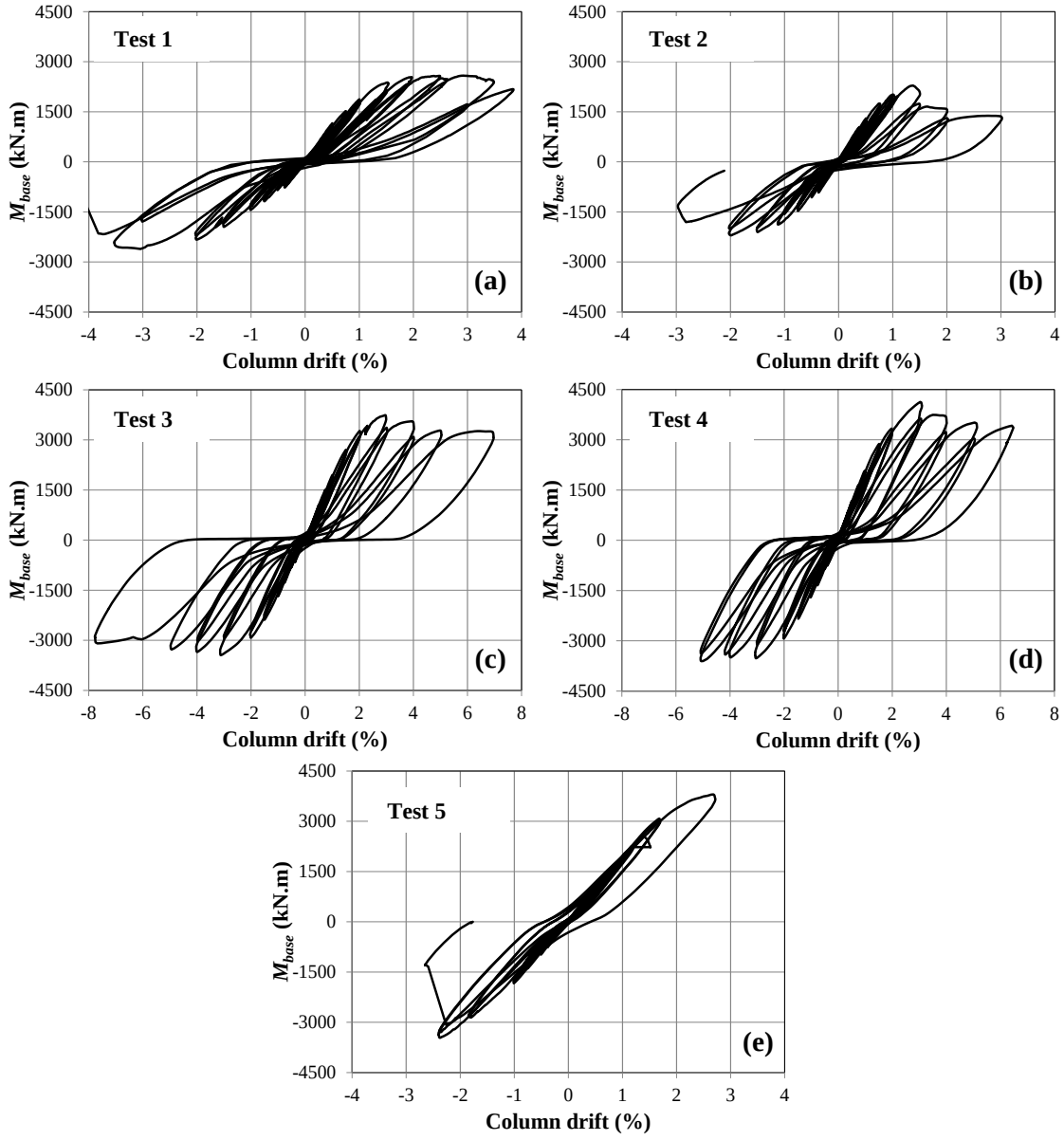

Fig. 3 – Moment drift plots for all experiments

In Test #1 and #2, with the shallower embedment final failure was accompanied by sudden uplift of a cone of concrete on the tension side of the connection (Fig. 4a). For Test #3 and #4 with the deeper embedment, failure was more gradual, as increasing deformations were accompanied by a steady drop in load. This results in a pattern of widespread cracking damage (as shown in Fig. 4b), in contrast with the sudden failure shown in Fig. 4a.

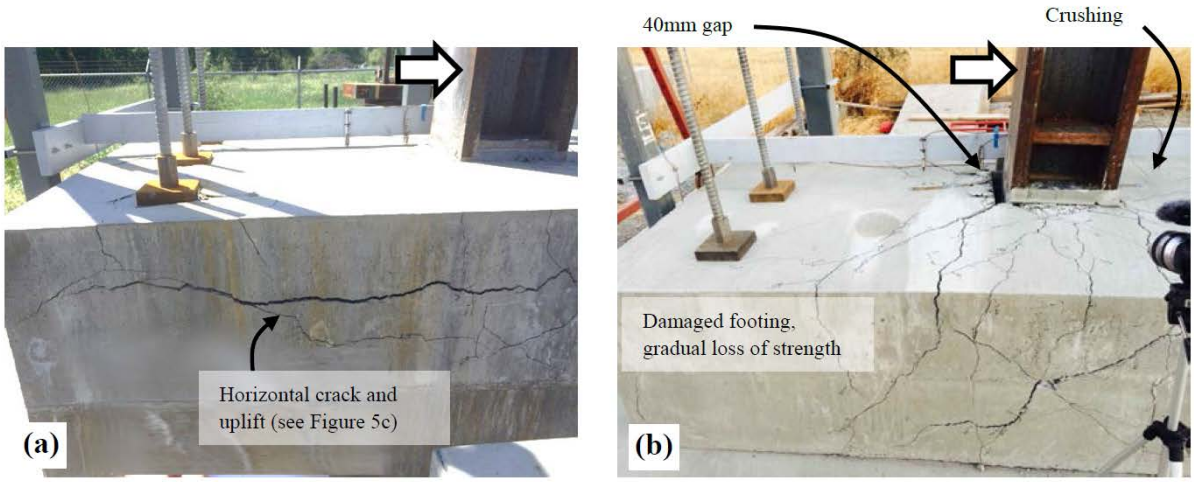

Fig. 4 – Failure patterns for tests with (a) shallower embedment and (b) deeper embedment

Based on the test results, and visual observations the physics of force transfer is postulated Fig. 5 illustrates the assumed physics. Referring to the Fig., it is assumed that compressive axial force is carried by the top stiffener plate, skin friction along the column, and the bottom base plate. Tensile axial force is carried by skin friction, and downward bearing on the bottom base plate. The base moment is resisted through a combination of horizontal bearing stresses against the flanges of the column (Fig. 5a) and vertical bearing stresses against the lower base plate (Fig. 5b). The horizontal bearing stresses are accompanied by shear in the panel zone. The tension field in the panel zone is responsible for the diagonal shear cracks observed in Fig. 4b. The strength model, described in the next section, is based on these mechanisms.

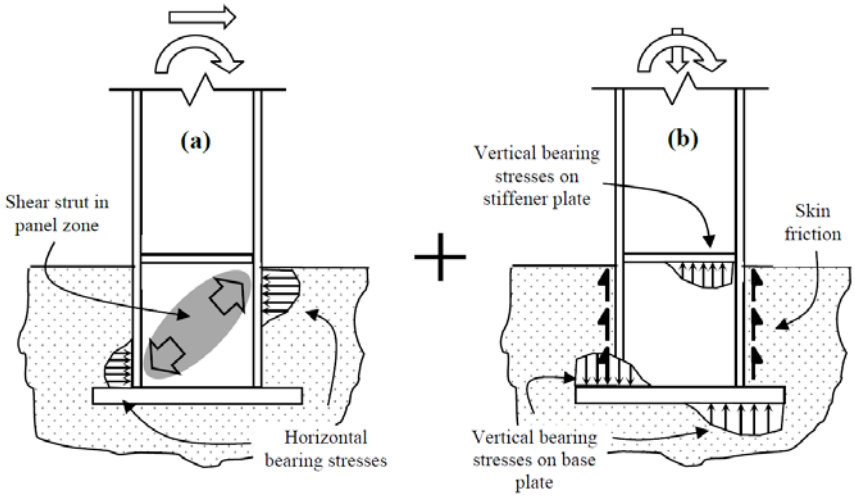

Fig. 5 – Force resisting mechanisms (a) horizontal bearing and panel zone strut (b) vertical bearing and skin friction

4. Strength Model

The strength model aims to characterize base moments associated with various limit states given the ECB geometry and applied axial force and shear to moment ratio. Specifically, the parameters defining the problem are: the column embedment depth d_{embed}, the column section, axial force P, base plate dimensions t_{plate}, B, N, and the shear–to–moment ratio, in addition to the dimensions of the footing as well as material properties of the steel of the base plate F_y^{plate} and the concrete, i.e., $f_c^{'}$.Given these parameters, the strength model determine must determine the base moments M_{base}, at which each of the possible limit states is attained, and finally determine the ultimate (or design) moment that can be sustained by the ECB connection.

The complete derivation and mathematical expressions for the strength model are significantly complex, and cannot be suitably described within the scope of this paper. The reader is directed to Grilli and Kanvinde (2015), as well as forthcoming journal articles on the topic. In this article, only the key aspects of the model and some equations are summarized. Fig.s 6a and b schematically illustrate the idealized internal forces associated with force and moment transfer from the column into the footing. Specifically, Fig. 6a shows compressive axial load transfer, and Fig. 6b shows moment and shear transfer.

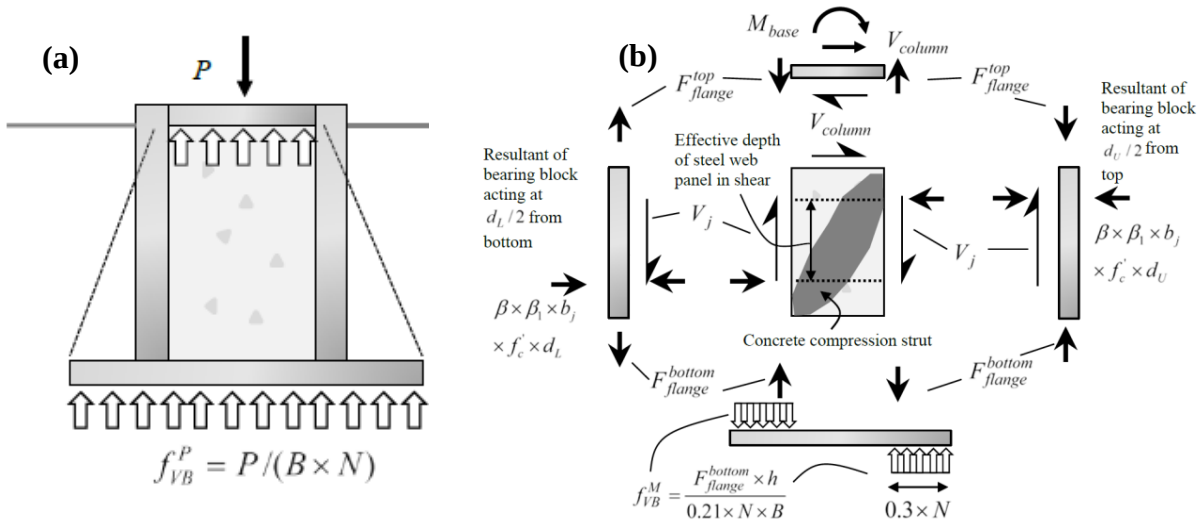

Fig. 6 – Internal force distribution with respect to (a) axial compression (b) shear and moment

Following the distribution shown in Fig. 6, the model assumes that the base moment may be decomposed into its components resisted by the horizontal and vertical bearing stresses, such that $M_{base} = M_{HB} + M_{VB}$. However, it is noted that this decomposition is an indeterminate one. To resolve this indeterminacy, it is further assumed that the net moment M_{base} is distributed in a constant proportion between the two mechanisms, such that –

$$M_{VB} = \alpha \times M_{base} \tag{1}$$

and,

$$M_{HB} = (1-\alpha) \times M_{base} \tag{2}$$

Where the ratio α controls the relative contribution of the two mechanisms. The contribution of the vertical bearing stresses will diminish as the embedment depth increases, since most of the moment will be carried by the horizontal bearing stresses; refer [5]. Once this is determined, a complex hierarchy of failure modes may be established. More specifically, the failure modes associated with the horizontal bearing are:

1. Bearing failure of concrete in front of the flanges.
2. Shear failure of the panel zone, including the strengths of the steel web, compression strut, and compression field.

Vertical bearing results in a different set of failure modes, as shown in Fig. 7a-d; these pertain to breakout of the concrete, yielding of the base plate and local crushing of the concrete near the base plate.

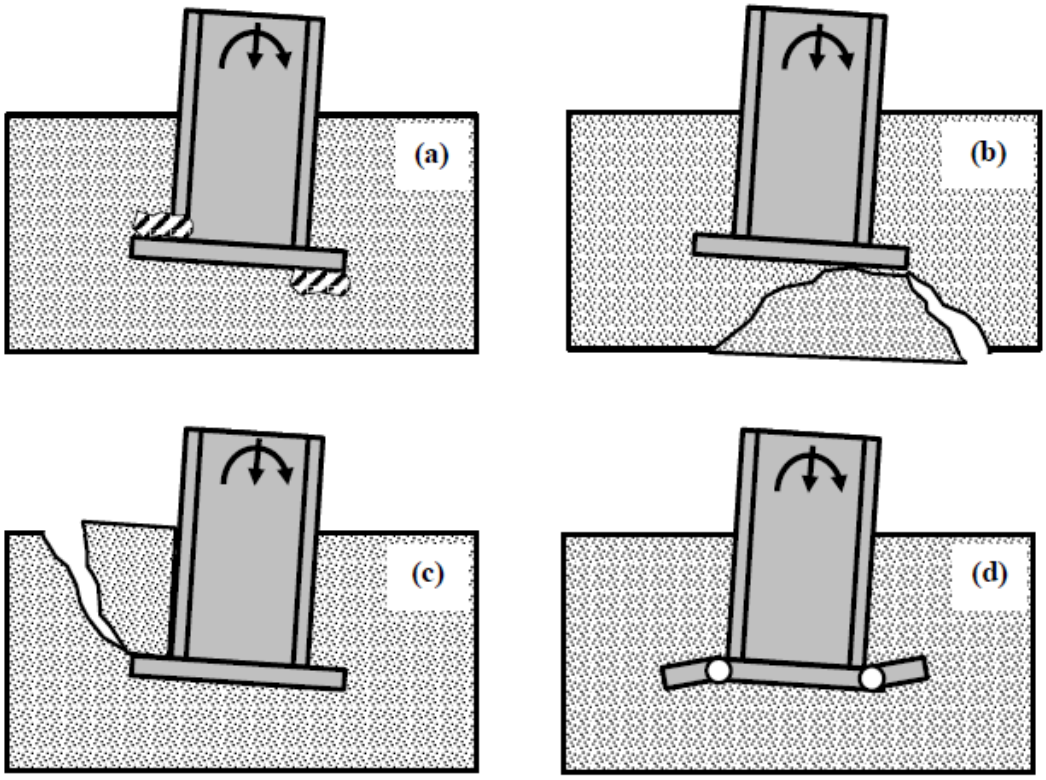

Fig. 7 – Limit states associated with vertical bearing (a) local crushing (b) and (c) breakout (d) base plate yielding

Once the strengths associated with each possible failure mode are determined, these need to be interpreted within a hierarchy of failure modes that interact in various ways. These interactions arise from (1) shared load paths between two failure modes (e.g., the compressive strut in the shear panel and bearing on the lower base plate), or (2) the nature of failure modes, e.g., some failure modes (horizontal bearing) are ductile allowing for the development of other limit states subsequent to them, whereas others are brittle (breakout of concrete due to vertical uplift) cause immediate loss in connection strength, with no possibility of further loading. The final strength method needs to recognize these interactions. The flowchart presented in Fig. 8 below shows a method for explicit consideration of these interactions in calculating connection strength – the terms are explained in greater detail in [5]; here only the overview is presented.

The method is inspired by physical observations of experimental response, but it is important to acknowledge, that some aspects of the method (coefficients in some formulas) have been empirically calibrated to achieve optimal agreement with test data. The resulting fit with test data is nearly perfect, with an average test to predicted ratio of 1.0, with a coefficient of variation of 6%.

4. Conclusions and Limitations

The study, and the strength method has many limitations, which must be considered in its interpretation and application. The limitations of the experimental program are inherited by the method as well – these include the examination of one generic detail, the absence of major reinforcement, and a relatively small data set for validation. Extrapolating the method to footing/embedment sizes that are significantly different from the method is potentially erroneous, since the empirical aspects of the method may be sensitive to size. It is also important to recall that the method only addresses failure modes that occur in the immediate vicinity of the embedded connection; and not those triggered by overall foundation failure. It is likely that these are sensitive to foundation type. Future work may involve additional experiments on different details, and finite element simulations for more accurate understanding of internal force transfer. Finally, the method provides deterministic estimates of nominal strength, and resistance $\phi-$ factors are required to ensure adequate margins of safety against failure. These may be developed through reliability analysis.

5. Acknowledgments

The authors are grateful to the Charles Pankow Foundation and the American Institute of Steel Construction for providing major funding for this project. Supplementary funding was provided by graduate fellowships at the University of California, Davis. Gregory Deierlein of Stanford University provided valuable feedback, as did Geoff Bomba of Forell Elsesser Enginers, and Ron Klemencic and Rob Chmielowski of Magnuson Klemencic Associates.

6. References

[1] Gomez, I.R., Kanvinde, A.M., Smith, C.M., and Deierlein, G.G., (2009), "Shear Transfer in Exposed Column Base Plates," Report Submitted to the American Institute of Steel Construction, Chicago, IL.

[2] DeWolf J.T., and Sarisley, E.F. (1980). “Column Base Plates with Axial Loads and Moments,” Journal of the Structural Division, ASCE, Vol. 106, No. 11, November 1980, pp. 2167-2184.

[3] Fisher, J.M. and Kloiber, L.A. (2006), “Base Plate and Anchor Rod Design,” 2nd Ed., Steel Design Guide Series No. 1, American Institute of Steel Construction, Inc., Chicago, IL.

[4] Grilli, D.A., and Kanvinde, A.M. (2013), “Special Moment Frame Base Connection: Design Example 8,” 2012 IBC SEAOC Structural/Seismic Design Manual, Volume 4, Examples for Steel-Frame Buildings, 255-280.

[5] Grilli, D.A. and Kanvinde, A.M. (2015). “Embedded Column Based Connections subjected to Flexure and Axial loads,” Report 3-11 submitted to the Charles Pankow Foundation.

[6] Krawinkler, H., Gupta, A., Medina, R., and Luco, N. (2000), “Loading Histories for Seismic Performance Testing of SMRF Components and Assemblies,” SAC Joint Venture, Report no. SAC/BD-00/10. Richmond, CA.